

# Verification of Planck's Law Through the Observation of Blackbody Spectra

Akhil Deshpande

PHY 353L Modern Laboratory  
Department of Physics  
The University of Texas at Austin  
Austin, TX 78712, USA

October 13, 2023

## Abstract

In our study, we employed a broadband prism spectrometer to gauge the spectral radiance from a blackbody source with temperatures between 600°C and 1100°C. Additionally, we derived values for the combined fundamental constants  $hc/k_B$  and the constant  $b$  in Wien's displacement law. Our results determine that the  $b$  in Wein's law had a value of  $2.98 \pm .04 \times 10^{-3}$  mK, and that our average value of  $\frac{hc}{k_B}$  was  $0.0148 \pm .0033$ . The data validated Planck's law and Wien's displacement law. Our  $hc/k_B$  measurement matched the known literature value, while our  $b$  value showed no significant deviation from existing literature.

## 1 Introduction

### 1.1 Physics Motivation

Blackbody radiation, a foundational concept in modern physics, emerged from the study of the spectrum of radiation emitted by objects as a function of temperature. Blackbody radiation refers to the electromagnetic radiation emitted by a perfect absorber - an object that absorbs all incident radiation - when it is in thermal equilibrium with its surroundings. The study of this radiation provides profound insights into the underlying principles of quantum mechanics and solidifies our understanding of the quantization of energy.

At the end of the 19th century, physicists relied heavily on classical physics to describe the behavior of physical systems. But the classical description of radiation emitted by a blackbody, based on Rayleigh-Jeans law, predicted that the energy radiated at short wavelengths (like ultraviolet) would become infinite, a problem famously known as the "ultraviolet catastrophe." Mathematically,

this can be expressed by the Rayleigh-Jeans law:

$$I(\nu) = \frac{8\pi\nu^2 k_B T}{c^3} \quad (1)$$

where  $I(\nu)$  is the intensity of radiation at frequency  $\nu$ ,  $k_B$  is the Boltzmann constant,  $T$  is the temperature of the blackbody, and  $c$  is the speed of light. As  $\nu$  approaches infinity, so does  $I(\nu)$ , leading to the aforementioned catastrophe.

It was Max Planck who, in a move of both brilliance and desperation, postulated that energy levels of oscillators in a blackbody were quantized, i.e., they could only take on certain discrete values. This was the birth of the quantization of energy, a concept alien to classical physics. Planck derived a new law of blackbody radiation which not only agreed with experimental results but also eliminated the ultraviolet catastrophe. Planck's law is given by:

$$I(\nu) = \frac{8\pi h \nu^3}{c^3} \frac{1}{e^{\frac{h\nu}{k_B T}} - 1} \quad (2)$$

where  $h$  is Planck's constant [1]. Planck's groundbreaking proposition led to the development of quantum mechanics. Five years later, in 1905, Einstein took Planck's idea of quantization of energy and applied it to the photoelectric effect, proposing that light itself could be considered as quantized in packets of energy, or photons. This work on the photoelectric effect, which further solidified the quantization principle proposed by Planck, earned Einstein the Nobel Prize in Physics in 1921 [3].

In essence, the study of blackbody radiation was instrumental in revealing the limitations of classical physics. It necessitated the development of a new theoretical framework — quantum mechanics. Without understanding blackbody radiation, the development of quantum mechanics, and hence our modern understanding of atomic and molecular phenomena, would be incomplete.

## 1.2 Historical context

The study of blackbody radiation is a journey that transcends more than a century, marked by both empirical observations and the theoretical underpinnings of quantum mechanics. Historically, the radiation emitted from a perfect blackbody, a body that absorbs and emits all radiation incident on it, was of considerable interest to physicists.

In the late 19th century, experimentalists first set out to chart the spectral intensity of blackbody radiation as a function of temperature. Traditional techniques deployed to measure the spectrum involved rudimentary devices like bolometers, which could gauge radiation by the changes in resistance of a fine wire. Lord Rayleigh and James Jeans famously predicted the intensity of such radiation at different wavelengths using classical physics, leading to the ultraviolet catastrophe. Their predictions significantly diverged from experimental data at shorter wavelengths.

The mismatch between the classical predictions and experimental results was the backdrop for Max Planck’s revolutionary proposition in 1900. Planck introduced the idea of quantized oscillators to explain the radiation curves, resulting in the Planck radiation formula, which aligned perfectly with experimental observations. This marked the birth of quantum mechanics, a realm where energy levels of oscillators are quantized.

As technology evolved, so did experimental techniques. One critical advancement was the realization that materials like metals could approximate a blackbody radiator if heated. This led to experiments wherein enclosed cavities in solid bodies were studied. Yet, as our apparatus description suggests, measuring the complete spectrum posed challenges both at lower and higher temperatures. While the lower temperature spectrum had minute radiance making it difficult to detect, ideal blackbody sources at higher temperatures were intricate to realize.

The inception of spectrometers brought about a paradigm shift in this realm. However, most early spectrometers, much like the grating spectrometers, were limited in their spectral range and calibration intricacies. It was not until the design of the prism spectrometer, reminiscent of our broadband prism spectrometer, that measurements became more precise. These spectrometers drew inspiration from the principle that different wavelengths of light refract at different angles through a prism, allowing for the isolation and measurement of specific wavelengths.

Our apparatus seems to be an ode to the early efforts in blackbody radiation measurement. The design, though sophisticated, mirrors the principles of the spectrometers first used for this purpose. The broadband prism spectrometer’s use of off-axis parabolic mirrors, a barium fluoride prism, and a thermopile detector echo the legacy of pioneering physicists, encapsulating a rich tapestry of both triumphs and tribulations. The rotating detector platform, an innovative touch, allows for the spectral range to be analyzed seamlessly, reminiscent of the pioneering spirit that has always characterized the realm of blackbody radiation experiments.

## 2 Theoretical background

The quest to understand the radiation emitted by a perfect blackbody has its roots deeply embedded in both classical and quantum physics. As we embark on this experiment, it’s crucial to provide a theoretical grounding.

The Planck Radiation Formula is the cornerstone of blackbody radiation theory. Originally postulated by Max Planck in 1900, this formula describes the spectral density of electromagnetic radiation emitted by a blackbody in thermal equilibrium. It is given by:

$$I(\nu, T) = \frac{8\pi h \nu^3}{c^3} \frac{1}{e^{\frac{h\nu}{kT}} - 1}$$

Where:

- $I(\nu, T)$  is the energy per unit volume per unit frequency interval.
- $h$  is Planck's constant  $\approx 6.626 \times 10^{-34}$  J s.
- $\nu$  is the frequency of the emitted radiation.
- $c$  is the speed of light in vacuum.
- $k$  is Boltzmann's constant  $\approx 1.381 \times 10^{-23}$  J/K.
- $T$  is the absolute temperature of the blackbody[4].

Another vital theoretical concept is Wien's Displacement Law. It states that the frequency ( $\nu_{\max}$ ) or wavelength ( $\lambda_{\max}$ ) at which the emission of a blackbody spectrum is maximized is inversely proportional to the temperature of the blackbody. Mathematically, it is expressed as:

$$\lambda_{\max} = \frac{c}{\nu_{\max}} = \frac{b}{T}$$

Where  $b$  is Wien's displacement constant, approximately  $2.898 \times 10^{-3}$  m K[5]. Lastly, the Stefan-Boltzmann Law provides a relation between the total emitted energy of a blackbody and its temperature. Given by:

$$E = \sigma T^4$$

Where:

- $E$  is the total emitted energy.
- $T$  is the absolute temperature.
- $\sigma$  is the Stefan-Boltzmann constant,  $5.67 \times 10^{-8}$  W m<sup>-2</sup>K<sup>-4</sup>[6].

As we conduct our measurements, it is these principles and equations that we rely upon to draw conclusions and inferences about the behavior of blackbody radiation. By understanding the theoretical underpinning of our experiment, we can provide a solid context to the observed results.

## 3 Experimental setup

### 3.1 Apparatus

In order to measure our blackbody spectrum, we used an already constructed broadband prism spectrometer. The spectrometer features an entrance slit, S1, and an exit slit, S2. Positioned before S1 is the radiation source. Radiation that moves through S1 encounters a 1-inch diameter off-axis parabolic mirror, M1, which is the Thorlabs model MPD169-P01. Ideally, M1 should be fully illuminated by the source. More specifics on this off-axis parabola can be found on its product website. The mirror's design is such that it takes in light from a

point source and emits a parallel beam devoid of any aberrations. The mirror boasts a reflected focal length of 6 inches and is structured for a right-angle reflection. It's crucial that the 6-inch gap between the slit and the mirror's center is accurately maintained, and the reflection angle should be nearly 90 degrees. The light beam from M1, which is parallel, is channeled to the in-



Figure 1: A vertical view of our spectrometer.

put face of a barium fluoride ( $\text{BaF}_2$ ) equilateral prism, with the part number BAFPRISM25.4-60 from Crystan Optics. This prism, with each side measuring 25.4 mm x 25.4 mm, bends the light, resulting in a parallel exit beam. This exiting beam is then caught by another off-axis parabolic mirror, M2, identical in design to M1. This mirror concentrates the light once again. Similar to M1, it's crucial for M2 to reflect at a 90-degree angle, and the arrow on its mounting bracket should be aligned with the parallel light rays.

Radiation that traverses slit S2 is detected by a thermopile detector (Dexter Research model 2M equipped with xenon fill gas, an internal thermistor, and a barium fluoride window). The detector features a 2 mm x 2 mm semiconductor "island", which constitutes its sensitive region. This island is anchored by a slender membrane with minimal thermal conductance. On this island, a sequence of tiny semiconductor thermocouple junctions is positioned, termed as "hot junctions". Another sequence of thermocouple junctions is affixed to a ceramic substrate connected to the device's casing, called the "cold junctions". These paired thermocouple arrays are configured to deductively measure the temperature variance between the hot and cold junctions. Positioned right behind a barium fluoride window is the sensitive region. Radiation passing through this window warms up the sensitive area, leading to a voltage emission from the apparatus that correlates with the power of the impinging radiation. The slit S2, mirror M2, and the detector are all affixed to a unified "detector platform". This platform is maneuverable via a motorized rotation stage (Newport Model URM100 PE). For a source emitting a singular wavelength, it's feasible to ad-

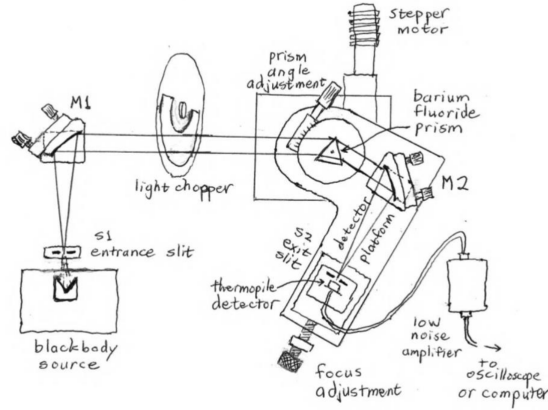


Figure 2: A sketch of our spectrometer.

just the platform's orientation such that the projection of S1 aligns with S2. Consequently, nearly all light transitioning through S1 also navigates through S2 and is captured by the detector. However, if the source's wavelength alters, the projection of S1 no longer aligns with S2 due to the prism's distinct angular deviation. Put simply, the detector perceives light with a singular angular deviation—or in essence, a single wavelength—at any given moment. This observed wavelength can be modified by rotating the detector platform, thereby directing rays with varied deviation angles onto the detector. By systematically varying the platform's angle across a spectrum, one can thus ascertain the detected power based on the wavelength, thereby determining the source's spectral distribution.

### 3.2 Data Collection

In order to collect data, we employed a method that was consistent and reliable each time with respect to the variance in our spectrometer setup. The main difficulties we faced were that the optics were not consistently aligned each time we began our experiment. By far, the most frustrating component was the thermopile detector. This detector sat on an extremely loose axis, and was easily nudged out of place. Therefore, we had a step by step routine each time we began to collect data. At the beginning of each lab day, we set up a 635nm laser, and conducted the following steps to ensure our spectrometer setup was consistent and accurate.

- Adjusted the prism angle adjustment to the angle that gave us the highest optical output.
- Adjusted the angle of the stage to match the minimum deflection angle of

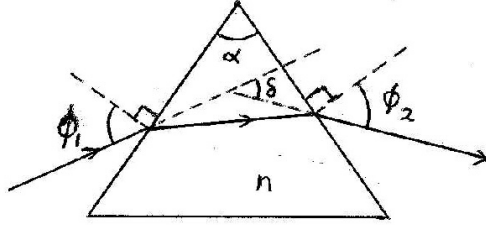


Figure 3: A diagram of how light rays are deflected in a prism.

our 635nm laser.

- Adjusted the thermopile detector to be in line with the stage.

Expanding on these bullet points, firstly, we rotated the prism's angle to find an angle that gave us the maximum optical output. This angle was measured once to be approximately  $154.5 \pm 1$  degrees. Then, using our 635nm laser again, we measured the output of the thermopile detector and amplifier, while changing the stage angle. When this output was maximized, we reset the angle the stage was at to 34.894 degrees, as this is the minimum deflection angle for a 60 degree prism, and light of 635nm.

Then, we began collecting data using our DAQ box and the blackbody source. Over intervals of 100 degrees Celsius, we rotated the stage from 29 degrees to 35 degrees. This was done to measure the intensity of the blackbody spectra as the angle varied. We began at a temperature of 600 degrees Celsius, and stopped at a temperature of 1100 degrees Celsius. The combined intensity versus angle graph is shown in Figure 4.

In Figure 4, we see a clear spike in the intensities at around 34 degrees for all of the temperatures.

### 3.3 Data Analysis

As stated in the lab manual, the main trouble with analyzing this data is that one cannot simply convert the angular deflection,  $\delta$  to the wavelength,  $\lambda$ . The reason for this is because the differential interval  $\Delta\delta$  is not equivalent to  $\Delta\lambda$ . Furthermore, another difficulty we are faced with is actually producing the inverted function  $\lambda(\delta)$  to convert from  $\delta$  to  $\lambda$  in our measured intensity spectrum. We obtained the latter function through interpolation. Since we have the angular deflection as a function of the index and the index as a function of wavelength, we can determine the angular deflection as a function of wavelength. From this,

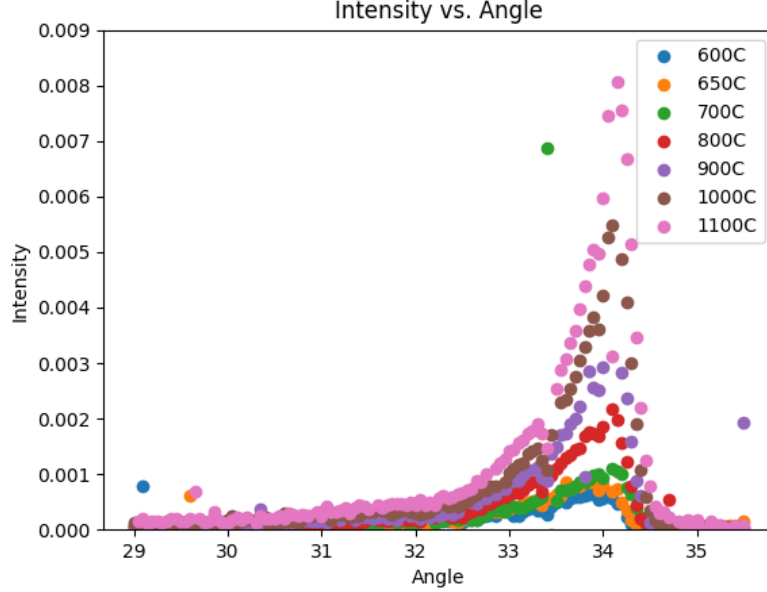


Figure 4: Combined Intensity vs. Angle data for all temps.

we interpolate (instead of finding the result analytically) in order to determine the inverse function. The relevant equations are found below.

$$n^2(\lambda) = 1.33973 + \frac{0.81070\lambda^2}{\lambda^2 - 0.10065^2} + \frac{0.19652\lambda^2}{\lambda^2 - 29.87^2} + \frac{4.52469\lambda^2}{\lambda^2 - 53.82^2} \quad (3)$$

$$\delta = \phi_1 + \arcsin(n \sin(\alpha - \arcsin(\sin \phi_1 n^{-1}))) - \alpha \quad (4)$$

Because we know that  $\alpha$  is 60 degrees, and  $\phi_1$  is 47.447 degrees, we can go ahead and calculate the inverse function  $\lambda(\delta)$ .

Our next step regards changing the intensity as a function of deflection angle to intensity as a function of wavelength. As discussed above, we cannot simply drop in our function for wavelength, as the differential intervals are different. To remedy this, we say that  $\lambda_i = \lambda(\delta_i)$ , and  $B(\lambda_i) = [B(\delta_i) * \frac{d\delta}{d\lambda}]|_{\lambda=\lambda(\delta_i)}$ . This calculation accounts for the disparity in differential intervals.

We then fit this data to Planck's Law (Equation 2), shown in Figure 5. Doing so, we were able to calculate the value of  $\frac{hc}{k_B}$ . Our average value of this quantity was  $0.0148 \pm .0033$ .

Furthermore, we conducted analysis on the Stefan-Boltzmann Law, as well as Wein's Law. The Stefan-Boltzmann Law is given by:

$$E = \sigma T^4 \quad (5)$$



where:

- $E$  is the energy radiated per unit area.
- $\sigma$  is the Stefan-Boltzmann constant,  $5.67 \times 10^{-8} \text{ W m}^{-2}\text{K}^{-4}$ .
- $T$  is the absolute temperature in Kelvin.

Wien's displacement law is given by:

$$\lambda_{\max} = \frac{b}{T} \quad (6)$$

where:

- $\lambda_{\max}$  is the peak wavelength.
- $b$  is Wien's displacement constant, approximately  $2.897 \times 10^{-3} \text{ m K}$ .
- $T$  is the absolute temperature in Kelvin.

Figures 6 and 7 show that our data supports Wein's Law and the Stefan-Boltzmann Law. We were able to determine that the  $b$  in Wein's law had a value of  $2.98 \pm .04 \times 10^{-3} \text{ mK}$

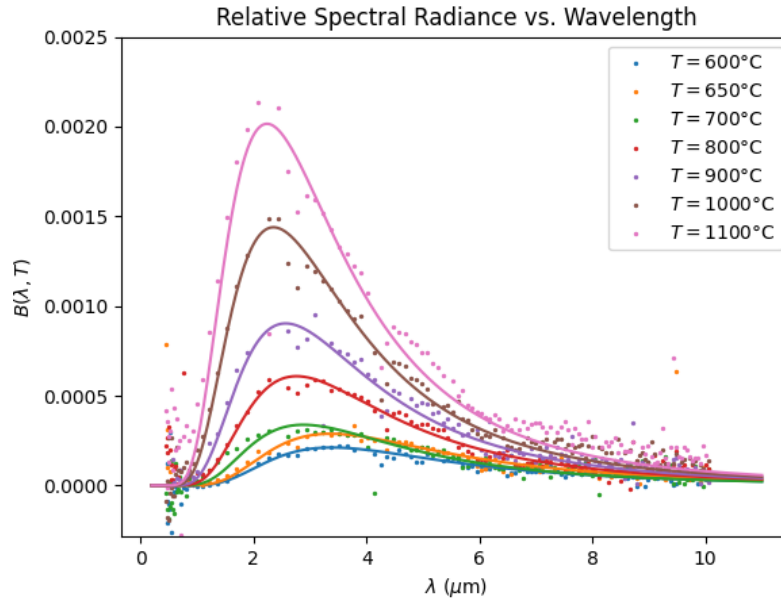


Figure 5: Combined Radiance vs. Wavelength data for all temps.

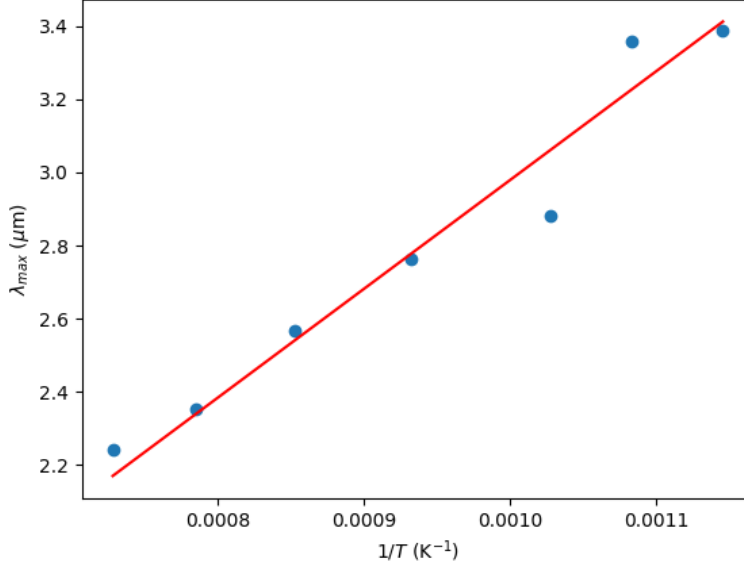


Figure 6: Wein's Law Fit.

## 4 Results

Figures 5, 6, and 7 all show good fits with their respective laws. However, in Figure 5, we see clear dips at around  $2.75\mu\text{m}$  and  $4.3\mu\text{m}$  in each of the temperature spectra. These dips correspond to the absorption spectrum of Carbon Dioxide, and are therefore an experimental anomaly, not one associated with Planck's Law. One way to combat this anomaly would be to try and conduct the experiment in a sort of vacuum chamber, or a chamber filled with a pure gas of known absorption spectra. Doing so would give a better and more clear view of the data, as that unknown variable would have been brought under control. We were able to determine that the  $b$  in Wein's law had a value of  $2.98 \pm .04 \times 10^{-3} \text{ mK}$ , and that our average value of  $\frac{hc}{k_B}$  was  $0.0148 \pm .0033$ .

## 5 Summary and conclusions

Our experiment made use of a broadband prism spectrometer equipped with a  $\text{BaF}_2$  equilateral prism. This setup allowed us to measure the relative spectral radiance emanating from a nearly ideal blackbody source at temperatures of 600, 650, 700, 800, 900, 1000, and  $1100^\circ\text{C}$ . The spectral radiance plots we obtained were in close alignment with the shape forecasted by Planck's law. Furthermore,

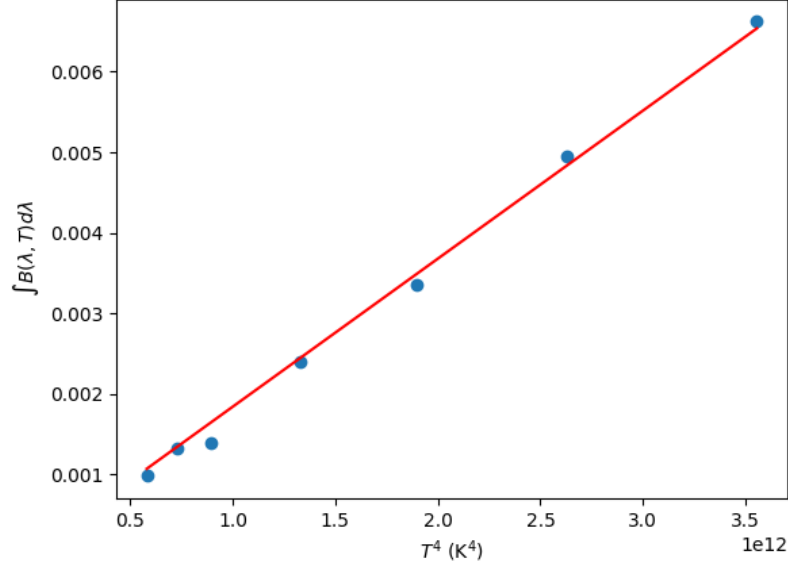


Figure 7: Stefan-Boltzmann Law Fit.

they showcased the linear relationship between  $\lambda_{\max}$  and  $\frac{1}{T}$  as proposed by Wien's law, as well as the linear correlation between the blackbody's radiance and  $T^4$ . From our data, we ascertained the value of  $\frac{hc}{k_B}$  to be  $(.0148 \pm .0033)$  m·K, and the b constant in Wien's law to be  $(2.98 \pm 0.04) \times 10^{-3}$  m·K. Our computed value for  $\frac{hc}{k_B}$  was consistent with the established literature, however, our value for b was not.

**Acknowledgments** I would like to thank my lab partner, Sannidhya Desai for his assistance on data collection. Furthermore, I'd like to thank Dr. Dan Heinzen, Parth Dave, and Konner Feldman for their assistance throughout the measurement and set up processes.

## References

- [1] Planck, M. (1901). "On the Law of Distribution of Energy in the Normal Spectrum". *Annalen der Physik*. 309 (3): 553-563.
- [2] Rayleigh, Lord (1900). "Remarks upon the Law of Complete Radiation". *Philosophical Magazine*. 49 (302): 539-540.

- [3] Einstein, A. (1905). “On a Heuristic Viewpoint Concerning the Production and Transformation of Light”. *Annalen der Physik*. 17: 132-148.
- [4] Max Planck. On the theory of the energy distribution law of the normal spectrum. *Verhandlungen der Deutschen Physikalischen Gesellschaft*, 2:237–245, 1900.
- [5] Wilhelm Wien. Über die Energieverteilung im Emissionsspektrum eines schwarzen Körpers. *Annalen der Physik*, 1896.
- [6] Ludwig Boltzmann. On the relationship between the second fundamental theorem of the mechanical theory of heat and probability calculations regarding the conditions for thermal equilibrium. *Sitzungsberichte der Kaiserlichen Akademie der Wissenschaften. Mathematisch-Naturwissenschaftliche Classe. Abt. II*, 76:373–435, 1877.